South African Journal of Botany 193 (2026) 311–322

Contents lists available at ScienceDirect

South African Journal of Botany

journal homepage: www.elsevier.com/locate/sajb

Hepatoprotective potential of *Vernonanthura polyanthes* against doxorubicin-induced oxidative stress in a murine model

Jamira Dias Rocha [a], Lara Lorhany Gomes da Costa Rodrigues [a], Hericles Mesquita Campos [b], Robbert Mota Pereira [b], Abel Vieira de Melo Bisneto [c], Samantha Salomão Caramori [a], Lee Chen-Chen [c], Paulo César Ghedini [b], Manoel Francisco Biancardi [d], Elisa Flávia Luiz Cardoso Bailão [a,*]

[a] Biotechnology Laboratory, Central Campus, State University of Goiás, Anápolis, Goiás, Brazil
[b] Department of Pharmacology, Institute of Biological Sciences, Federal University of Goiás, Goiânia, GO, Brazil
[c] Radiobiology and Mutagenesis Laboratory, Federal University of Goiás, Goiânia, Goiás, Brazil
[d] Department of Histology, Embryology and Cell Biology, Federal University of Goiás, Goiânia, Goiás, Brazil

ARTICLE INFO

Edited by Dr P. Bhattacharyya

Keywords:
4-hydroxynonenal labeling
Adriamycin
Antioxidant effect
Assa-peixe
Cerrado
Lipid peroxidation

ABSTRACT

The present study aimed to evaluate the redox activity of *Vernonanthura polyanthes* leaf aqueous extract (*Vp*LAE) and its n-butanol fraction (n-BF) in mouse liver in the absence or in the presence of doxorubicin (DXR). For this, the concentration of malondialdehyde (MDA), the activities of superoxide dismutase (SOD), catalase (CAT), glutathione S-transferase (GST), and glutathione peroxidase (GPx) were determined in the liver of Swiss Webster mice (n = 5 animals *per* group). Immunohistochemical analyses on hepatocytes labeled with anti-4-hydroxynonenal (4HNE) were also performed to confirm the decrease in lipid peroxidation in animals treated with DXR and *Vp*LAE or n-BF. MDA levels and GST activity increased in the livers of mice that received just *Vp*LAE at a dose of 1000 mg/kg compared with the negative control. Moreover, n-BF alone increased CAT activity at 250 mg/kg, SOD and GST at 1000 mg/kg, and MDA at 250, 500, and 1000 mg/kg. These data indicate that *Vp*LAE or n-BF alone can promote oxidative stress in hepatocytes. In contrast, when *Vp*LAE was associated with DXR in a pre-treatment regimen, or when n-BF was associated with DXR in co- or pre-treatment regimens, MDA levels decreased, suggesting a protective effect against DXR-induced damage. The decrease in 4HNE labeling in the livers of mice treated with DXR and *Vp*LAE or n-BF confirmed that pre-treatment with *Vp*LAE or pre- and co-treatments with n-BF reduced DXR-induced lipid peroxidation. In conclusion, *Vp*LAE and n-BF could present a dual behavior, promoting oxidative stress in hepatocytes in the absence of DXR or reducing oxidative stress in the livers of mice treated with DXR. This shift in perspective motivates future studies of *Vp*LAE and n-BF as promising candidates to overcome DXR-induced hepatotoxicity.

1. Introduction

Doxorubicin (DXR), an anthracycline drug, is an antineoplastic agent widely used to treat hematologic tumors and solid malignancies, including leukemias, bladder cancer, lung cancer, breast cancer, ovarian cancer, and lymphomas (Guo et al., 2014; Wattanapitayakul et al., 2005). There are two proposed pharmacological mechanisms of DXR: (i) intercalation into DNA and disruption of topoisomerase-II-mediated DNA repair and (ii) generation of free radicals (Thorn et al., 2011). These free radicals can cause lipid peroxidation of cell membranes, protein damage, changes in mitochondrial function, and DNA breaks (Octavia et al., 2012; Prasanna et al., 2020; Singal and Iliskovic, 1998). The adverse effects of DXR are caused, in part, by an imbalance in the body's redox system, promoting cellular damage and increased production of free radicals, as well as a decrease in endogenous antioxidants, which can lead to toxicity in different organs and tissues, including the liver (Singal et al., 2000; Xu et al., 2001). Moreover, DXR disrupts normal cellular iron metabolism, leading to excessive iron accumulation and the formation of reactive oxygen species (ROS) via the Fenton reaction (Ye et al., 2024).

* Corresponding author at: Laboratório de Biotecnologia, Câmpus Central, Universidade Estadual de Goiás, Anápolis, BR-153, n. 3105, Fazenda Barreiro do Meio, CEP 75132-903, Goiás, Brazil.
E-mail address: elisa.flavia@ueg.br (E.F.L.C. Bailão).

https://doi.org/10.1016/j.sajb.2026.04.014
Received 1 December 2025; Received in revised form 23 March 2026; Accepted 9 April 2026
Available online 28 April 2026

In this sense, although DXR is a highly effective chemotherapeutic agent, its clinical use is hampered by its toxic effects on non-target cells (Forrest et al., 2012; Prasanna et al., 2020). An injectable DXR may be the primary cause of hepatotoxicity in approximately 30.4% of breast cancer patients treated with this drug, since there is a strong correlation between the use of injectable DXR and the risk of developing hepatotoxicity (Damodar et al., 2014; Shivakumar et al., 2012).

Several signaling pathways have been proposed to underlie DXR-induced hepatotoxicity, including mitochondrial dysfunction, redox imbalance, and cell death (Alherz et al., 2023; Prasanna et al., 2020). Following administration, DXR is metabolized to doxorubicinol by liver tissue, which can cause severe liver damage, usually due to the formation of ROS (Camaggi et al., 1988; Rehman et al., 2014). DXR undergoes redox cycling, creating superoxide radicals that destroy cellular structures, initiate lipid peroxidation, and trigger cell death pathways (Songbo et al., 2019). In this context, oxidative stress, primarily driven by excessive mitochondrial ROS generation, is the primary mechanism of DXR hepatotoxicity.

Strategies to protect against DXR-induced hepatotoxicity and improve the effectiveness of therapies have been extensively studied (Radeva and Yoncheva, 2025). The use of liposomal DXR or the restriction of cumulative doses often fails to completely eliminate liver damage and may interfere with the drug's antitumor efficacy (Radeva and Yoncheva, 2025). Administration of natural products rich in non-enzymatic antioxidants may be a potential strategy for preventing or mitigating oxidative stress, including DXR-induced damage (Aguiar et al., 2024; Rocha et al., 2022; Samare-Najaf et al., 2020; Wattanapitayakul et al., 2005). Phenolic compounds and flavonoids demonstrated strong cytoprotective effects against DXR-induced side effects, including hepatotoxicity (Abbas et al., 2021; Cheng et al., 2022; Halil et al., 2021; Rocha et al., 2022). Plant extracts exhibit varying degrees of hepatoprotective properties, suggesting that antioxidants from natural sources may help protect against hepatotoxicity in patients receiving DXR (Damodar et al., 2014; Mahmoudi et al., 2023). However, it is important to highlight the ambivalent properties of polyphenols, which can act simultaneously as antioxidants and pro-oxidants. Understanding this dual role will enable the development of specific therapies that can serve science and medicine (Andrés et al., 2023).

Vernonanthura polyanthes (Spreng.) A.J. Vega & Dematt. belongs to the Asteraceae family and is popularly known as assa-peixe. It is an emerging invasive alien plant found in a Zimbabwean upland landscape (Kachena and Shackleton, 2024). Its leaves are widely used in traditional medicine to treat respiratory tract diseases (Chaves et al., 2015; Lorenzi and Matos, 2002; Tribess et al., 2015). Recently, it has been shown that the aqueous extract of *V. polyanthes* leaves (*Vp*LAE) and its n-butanol fraction (n-BF) can reduce the cytogenotoxic effects caused by DXR (Rocha et al., 2022). The cytoprotective effect of *V. polyanthes* may be related to its phytochemical composition, as flavonoids and chlorogenic acids were identified in *Vp*LAE and n-BF (Rocha et al., 2022). Potential antimutagenic, anticancer, antineoplastic, chemoprotective, antioxidant, and free-radical-scavenging effects were attributed to metabolites identified in *Vp*LAE and n-BF through predictive analysis (Rocha et al., 2022). Some molecules identified in *Vp*LAE and n-BF have been shown to modulate enzymes involved in antioxidant processes. Among the metabolites detected in *Vp*LAE and n-BF, quercetin-3-O-rutinoside (rutin) appears to be the most active, based on the antioxidant and chemopreventive parameters analyzed using in silico tools (Aguiar et al., 2024; Rocha et al., 2022).

However, the effects of *V. polyanthes* on the liver tissue remain unknown. Therefore, this study aimed to evaluate the redox activity of

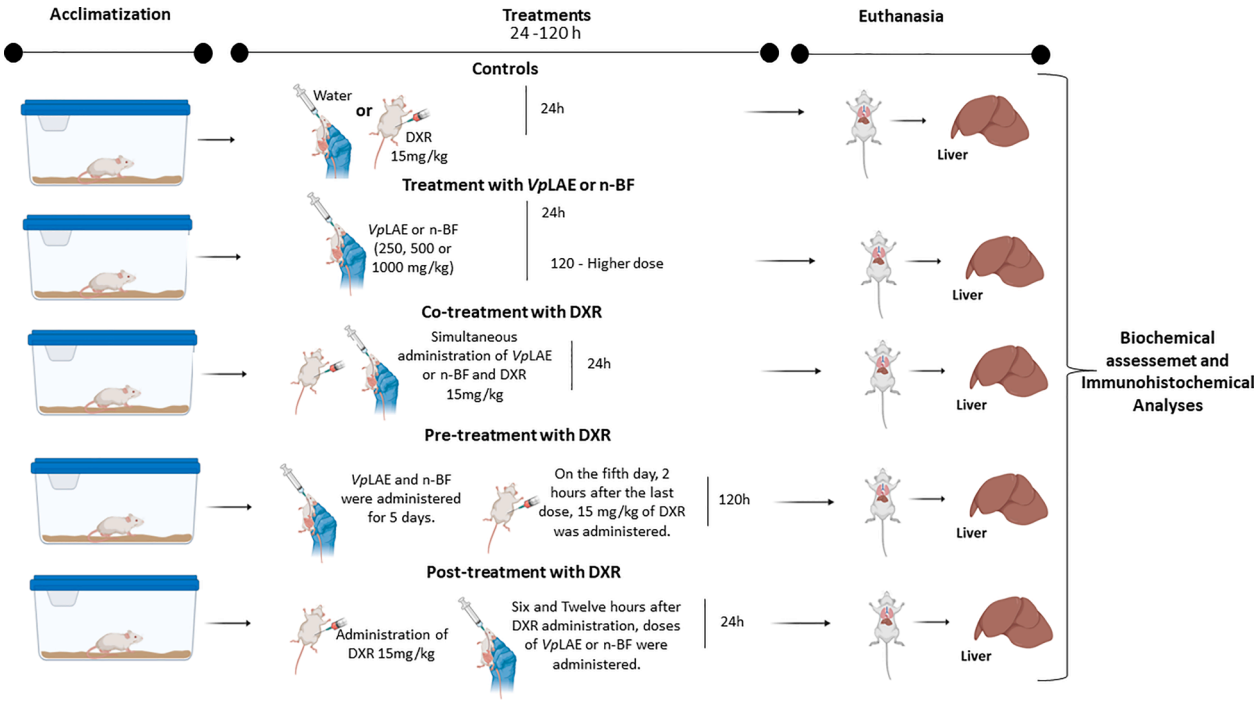

Fig. 1. Schematic illustration of the experimental design. After acclimatization, the animals were then randomly distributed into 28 groups (n = 5 animals per group). The control groups received water by gavage or 15 mg/kg doxorubicin (DXR) i.p., and after 24 h the animals were euthanized. The groups that received doses of 250, 500, or 1000 mg/kg of aqueous extract of *Vernonanthura polyanthes* (*Vp*LAE) or its n-butanol fraction (n-BF) alone were euthanized after 24 h of treatment. The co-treatment groups received 250, 500, or 1000 mg/kg of *Vp*LAE or n-BF and 15 mg/kg DXR i.p., and the animals were euthanized after 24 h. The pre-treatment was carried out by administering 250, 500, or 1000 mg/kg of *Vp*LAE or n-BF for 5 days (one dose per day), and on the fifth day, the animals received 15 mg/kg DXR i.p., and 24 h later, the animals were euthanized. The post-treatment groups received 15 mg/kg DXR i.p., and after 6 and 12 h, received 250, 500, or 1000 mg/kg of *Vp*LAE or n-BF, and 24 h later, the animals were euthanized. After euthanasia, the liver was dissected and immediately conserved in liquid nitrogen and, subsequently, in an ultrafreezer (−80 °C) until the biochemical analysis, or fixed in formaldehyde solution (10%) for 24 h to immunohistochemical analysis. The components of the figure were created using icons from the online design tool BioRender (https://www.biorender.com).

*Vp*LAE and n-BF in the livers of Swiss Webster mice in the absence or presence of DXR. The hypothesis is that *Vp*LAE and n-BF are potential candidates to mitigate DXR-induced hepatotoxicity.

2. Methodology

2.1. Chemicals

1-chloro-2,4-dinitrobenzene (CDNB), hydrogen peroxide (H_2O_2), sodium azide, reduced glutathione (GSH), nicotinamide adenine dinucleotide phosphate (NADPH), glutathione reductase (GR), trichloroacetic acid, ketamine, xylazine hydrochloride, epinephrine bitartrate, malondialdehyde (MDA), bovine serum albumin (BSA) and sodium dodecyl sulfate (SDS) were obtained from Sigma Chemical (St. Louis, MO, USA). Doxorubicin (DXR) (CAS: 23214-92-8) was obtained from Glenmark Pharmaceuticals LTDA (São Paulo, BRA). All other chemicals were obtained in an analytical grade or from other standard commercial suppliers.

2.2. Botanical material

V. polyanthes leaves were collected at the Central Campus, in Anápolis, Goiás, Brazil (S 16 2300.16″/W 48 56,037.8″, 1073 m) in November 2018. The botanical identification of this specimen was carried out by Dr. Aristônio Magalhães Teles from the Federal University of Goiás, and an exsiccate (N° 10,512) was deposited in the Herbarium of the State University of Goiás. The botanical material was dried at room temperature and pulverized in a knife mill E-625 (Tecnal Ltda, Piracicaba, SP, Brazil). The powdered material was stored in a sheltered location to protect it from light and moisture for subsequent use. According to popular usage, the aqueous extract was prepared by infusing *V. polyanthes* leaves at a ratio of 0.02 g of dried and pulverized plant material per mL of water (Brasil, 2011). The samples were previously frozen and lyophilized. Part of the lyophilizate was reconstituted in a methanol/water mixture and subjected to liquid/liquid partitioning with solvents of increasing polarity (n-butanol and ethyl acetate). After rotary evaporation, three fractions (n-butanol, ethyl acetate, and aqueous) were obtained and stored at −20 °C for biological testing (Rocha et al., 2020). The n-BF was selected to continue the experiments because it exhibited the highest total phenolic, flavonoid, and tannin contents and the highest antioxidant activity, according to previous work (Rocha et al., 2020). The chemical profiles of *Vp*LAE and n-BF were previously evaluated by liquid chromatography coupled to mass spectrometry, confirming the presence of phenolic compounds (flavonoid and chlorogenic acids) (Rocha et al., 2022).

2.3. Selection of doses used in this study

The doses were selected from the study by Jorgetto et al. (2011), which tested 3 doses (1000, 1500, and 2000 mg/kg body weight) of *V. polyanthes* extract, in accordance with OECD 423 (OECD, 2001). The results showed that the *V. polyanthes* extract presented moderate clastogenic and/or aneugenic effects at 2000 mg/Kg. In this sense, we decided to limit our study to the lowest dose used by Jorgetto et al. (2011) (1000 mg/kg). Thus, doses of 250, 500, and 1000 mg/kg of *Vp*LAE or n-BF were selected for this study, as previously described (Rocha et al., 2022).

2.4. In vivo experimental procedures

The experiments with male *Mus musculus* (Swiss Webster) were approved by the Animal Research Ethics Committee of the Federal University of Goiás (CEUA/UFG), protocol number 069/18, and were carried out as previously described (Rocha et al., 2022). Before conducting the experiments, the animals were acclimated for 7 days in the Radiobiology and Mutagenesis Laboratory at the Federal University of Goiás (Fig. 1). The animals were housed in polypropylene cages (Length: 40 cm, Width: 30 cm, and Height: 16 cm), with 5 animals in each cage. The cages were lined with wood shavings, which were changed every two days, and the animals were fed commercial food and offered filtered water *ad libitum*. The animals were maintained at room temperature, with a humidity of 50% ± 20%, and a 12 h light/dark cycle. The animals were divided into 28 groups, as previously described (Rocha et al., 2022; Silva et al., 2023), each containing five mice, in accordance with OECD 474 (OECD, 2016). The animals were weighed before the administration of *Vp*LAE or n-BF at doses of 250, 500, and 1000 mg/kg via gavage with or without DXR (15 mg/kg) intraperitoneally (ip) (Fig. 1 and Supp. Table S1), as indicated below:

- ***Group 1, negative control:*** received water via gavage in the same volume used to administer *Vp*LAE or n-BF.
- ***Group 2, positive control:*** received an acute dose of DXR (15 mg/kg) ip. Selected based on the study by Husna et al. (2022), which highlighted the hepatotoxicity of the drug.
- ***Groups 3 to 10, treatment:*** received only *Vp*LAE or n-BF by gavage in different doses (250, 500, or 1000 mg/kg).
- ***Groups 11 to 16, co-treatment:*** received *Vp*LAE or n-BF (250, 500, or 1000 mg/kg) via gavage simultaneously with 15 mg/kg DXR via ip.
- ***Groups 17 to 22, pre-treatment:*** received *Vp*LAE or n-BF (250, 500, or 1000 mg/kg) for 5 days (120 h), and on the fifth day, two hours after administration of *V. polyanthes*, received 15 mg/kg DXR via ip.
- ***Groups 23 to 28, post-treatment:*** received 15 mg/kg DXR ip and after 6 h and 12 h, received *Vp*LAE or n-BF (250, 500, or 1000 mg/kg) via gavage.

After the treatment, the animals were euthanized by cervical dislocation. The liver was dissected and immediately conserved in liquid nitrogen and, subsequently, in an ultrafreezer (−80 °C) until the biochemical analysis, or fixed in formaldehyde solution (10%) for 24 h to immunohistochemical analysis.

2.5. Sample preparation for biochemical analysis

For the biochemical analysis, the liver samples were homogenized in 50 mM Tris–HCl buffer (pH 7.4) at a 1:6 (w/v) sample-to-buffer ratio. The total homogenate (TH) was centrifuged at 8000 rpm for 10 min at 4 °C to acquire the low-speed supernatant (S1). Both the TH and S1 fractions were preserved and used in subsequent biochemical procedures.

2.6. Superoxide dismutase (SOD) activity

SOD activity was determined spectrophotometrically. The principle of this method is that the enzyme superoxide dismutase inhibits the autoxidation of epinephrine. The S1 liver fractions were incubated with 60 mmol/L epinephrine bitartrate, and the color intensity of the sample was measured at 480 nm. Enzymatic activity is expressed in units (U) of SOD/mg of protein (Campos et al., 2024).

2.7. Catalase (CAT) activity

CAT activity was determined spectrophotometrically by decomposing H_2O_2 at 240 nm, as described by Campos et al. (2024). The S1 liver fractions were incubated with 86 mmol/L H_2O_2 in sodium phosphate buffer (pH 7.0). Enzymatic activity is expressed in U of CAT/mg of protein. One U of enzyme decomposes 1 μmol of H_2O_2/min at pH 7.0 at 25 °C.

2.8. Glutathione peroxidase (GPx) activity

GPx activity was determined using the method described by Okoh et al. (2024), with some modifications. The following reagents were

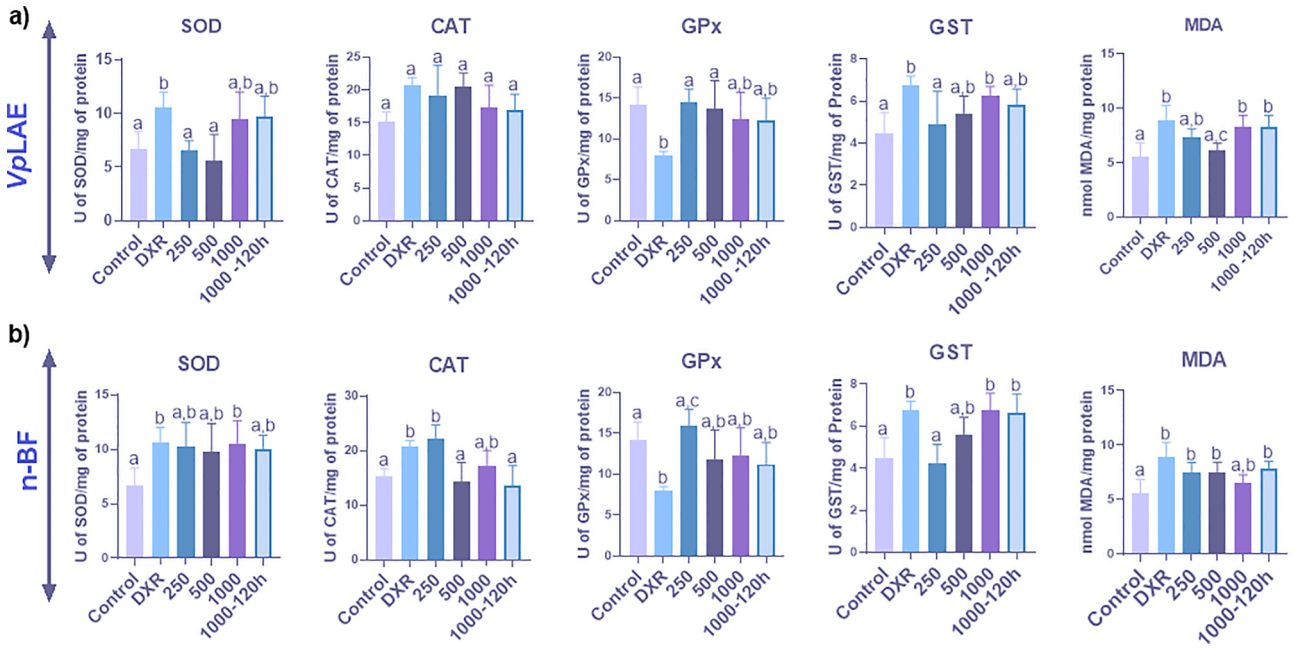

Fig. 2. Biochemical alterations in the liver of mice treated with different doses (250, 500, and 1000 mg/kg) of the (a) *Vernonanthura polyanthes* leaf aqueous extract (*Vp*LAE) or the (b) n-butanol fraction (n-BF). Control: negative control (mineral water). DXR: positive control (doxorubicin 15 mg/kg ip). The results are expressed as mean ± standard deviation. The groups were compared by ANOVA followed by the Tukey test (n = 5 animals per group). Different letters indicate statistically significant differences between groups ($p < 0.05$). The abbreviations SOD, CAT, GST, GPx, and MDA mean superoxide dismutase, catalase, glutathione S-transferase, glutathione peroxidase, and malondialdehyde, respectively.

added to the reaction medium: 4.28 mM sodium azide, 6 mM GSH, 0.9 mM NADPH, 2 U/ml GR, phosphate buffer 50 mM potassium. The S1 liver fractions or Tris–HCl buffer (blank) were added and, to start the reaction, 4 mm of H_2O_2 was added. Activities were evaluated over 5 min at 340 nm, with measurements taken every 15 s. Enzymatic activity was expressed as GPx activity (U/mg protein). One U of enzyme will thus decompose 1 μmol of NADPH/min at pH 7.0 and 25 °C.

2.9. Glutathione S-transferase (GST) activity

GST activity was determined using the method described by Kato and Naito (1999), with some modifications. S1 liver fractions were added to Tris–HCl buffer (white), 50 mM CDNB dissolved in methanol, and 5 mM GSH dissolved in 100 mM Tris–HCl (pH 7.0). Reactions were monitored every 15 s for 5 min at 340 nm. The concentration of the product formed was calculated using the molar extinction coefficient of 9.6 mM-1.cm-1 for S-(2,4–dinitrophenyl glutathione). Specific activity will be defined as U of GST/mg of protein. One U of enzyme conjugates 1 μmol of CDNB/min at pH 7.0 and 25 °C.

2.10. Levels of lipid peroxidation (LPO)

To measure LPO, the thiobarbituric acid reactive substances (TBARS) method was used. MDA estimation was performed spectrophotometrically following the method described by Campos et al. (2024). The liver TH samples were incubated with thiobarbituric acid, acetic acid (pH 3.4), and SDS at 95 °C for 60 min. The reaction product was determined at 532 nm. To interpret the results, an MDA curve was performed, and the data are expressed as MDA equivalents in nmol /mg of protein.

2.11. Determination of protein content

The total protein concentration of TH or S1 fractions was measured using the method described by Bradford (1976), with BSA as the standard. A BSA standard curve was used to determine the protein concentration in the samples.

2.12. Immunohistochemical: detection of 4-hydroxynonenal (4HNE) protein adducts

The livers fixed in formaldehyde solution (10%) for 24 h were gradually dehydrated in increasing alcohol solutions (70%, 80%, and 95%) for 1 h each step and then in absolute alcohol three times for 1 h each. Subsequently, the tissues were cleared with xylene for 2 h and then immersed in paraffin.

Right away, the histological sections (30 sections/experimental group; n = 5 animals/group) of the livers, fixed in 10% formaldehyde, were deparaffinized in three xylene batteries, the first lasting 20 min and the other two lasting 10 min, followed by rehydration. Subsequently, the sections were subjected to antigen recovery in citrate buffer pH 6.0 at 100 °C for 45 min in an electric cooker. Next, the sections were washed thrice in phosphate-buffered saline (PBS) for 5 min each. From this stage onwards, the Leica Biosystems NovoLink Polymer Detection System kit (RE7150-K, Leica, United Kingdom) was used to detect the primary antibodies. Thus, endogenous peroxidases were blocked using Novoastra Peroxidase Block for 5 min, and the sections were then washed 3 times in PBS for 5 min each. Non-specific binding was inhibited using Novocastra protein block for 5 min, followed by 3 washes of 5 min in PBS. Then, the polyclonal anti-4-hydroxynonenal (4HNE) primary antibody (Rabbit polyclonal, BS-6313R, Bioss, USA) was used at a dilution of 1:100 and incubated overnight at 4 °C. The following day, the sections were washed three times in PBS for 5 min each and incubated with secondary antibodies Novocastra Post Primary and Novolink Polymer, both for 1 h at room temperature, with three 5-minute washes in PBS buffer interspersed between incubations. Finally, the sections were developed with diaminobenzidine (DAB), counterstained with Harris hematoxylin, dehydrated in ethanol, followed by xylene, and mounted in Entellan (Merck). Microscopic analysis was conducted using an optical microscope (Primo Star, Carl Zeiss), and photomicrographs were captured with a camera module (Axiocan 105 color, Carl Zeiss).

4-hydroxynonenal (4HNE) was quantified using 30 microscopic fields (n = 5 animals per group) for each experimental group. In each field, optical densitometry was used to measure immunostaining

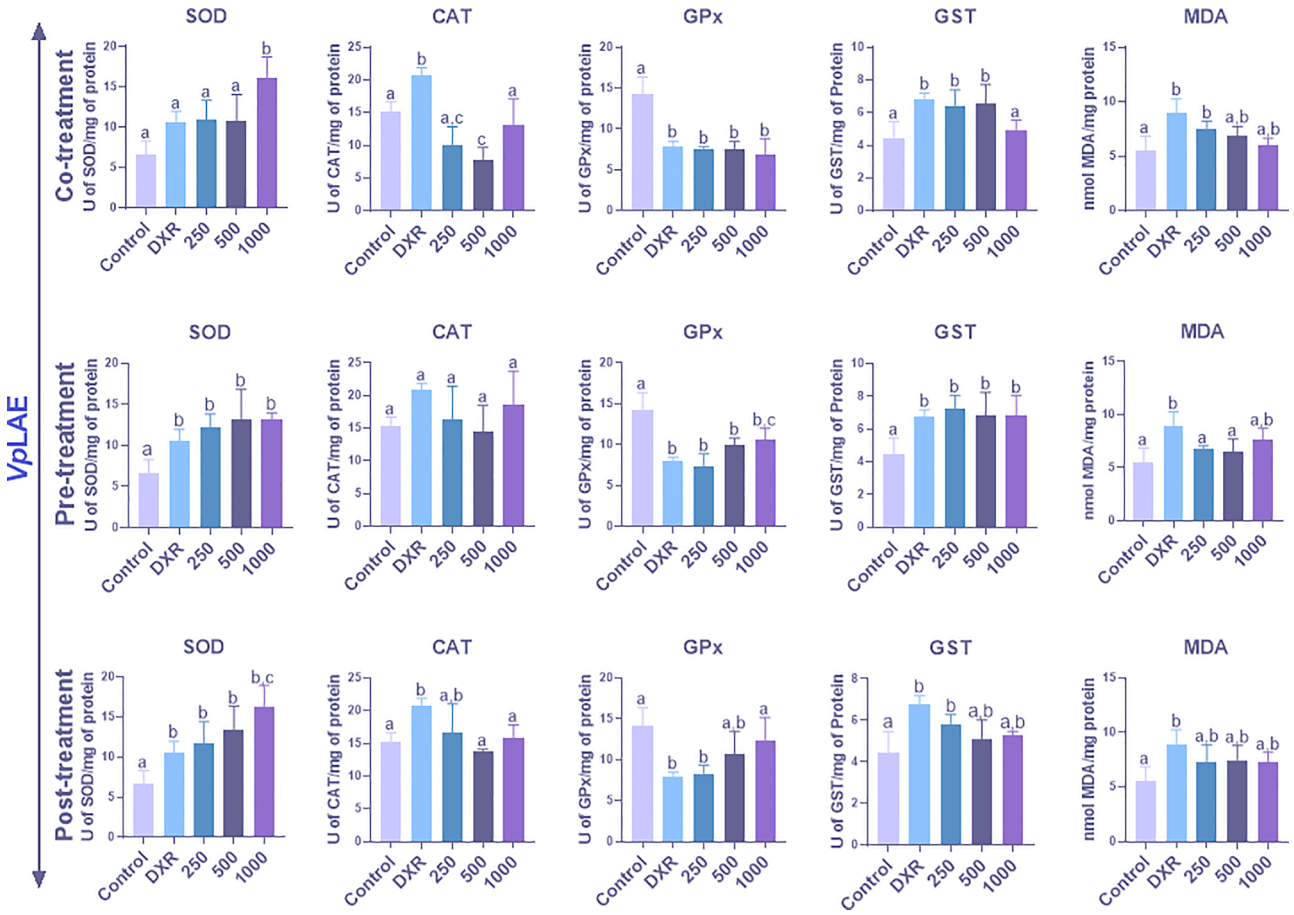

Fig. 3. Biochemical changes in the liver of mice treated with different doses (250, 500, and 1000 mg/kg) of the aqueous extract of the leaves of *Vernonanthura polyanthes* (*Vp*LAE) associated with doxorubicin (DXR) in several different treatments. Control: negative control (mineral water) and DXR: positive control (doxorubicin 15 mg/kg ip). The results are expressed as mean ± standard deviation. The groups were compared by ANOVA followed by Tukey's test (n = 5 animals per group). Different letters indicate statistically significant differences between the groups ($p < 0.05$). The abbreviations SOD, CAT, GST, GPx, and MDA mean superoxide dismutase, catalase, glutathione S-transferase, glutathione peroxidase, and malondialdehyde, respectively.

intensity. We used the "mean gray value" measurement for quantification, and the system was calibrated with the optical density tablet. Since the original images were counterstained with hematoxylin, we used color deconvolution to obtain the 3,3′-diaminobenzidine (DAB) channel to quantify staining intensity (optical density, OD), expressed in arbitrary units (au). All analyses were performed using the Fiji/ImageJ image analysis system (Schindelin et al., 2012).

3. Results

3.1. Biochemical analysis of liver from mice treated with Vernonanthura polyanthes leaf aqueous extract (VpLAE) or its n-butanol fraction (n-BF) alone

The GST activity (in 24 h) and the quantity of MDA (in 24 and 120 h) increased in the liver of mice that received *Vp*LAE at the highest dose (1000 mg/kg) when compared to the negative control (Fig. 2A). On the other hand, the n-BF increased the SOD and the GST activities at 1000 mg/kg (in 24 h for SOD, and 24 e 120 h for GST), the CAT activity at 250 mg/kg, and the MDA quantity at 250 and 500 mg/kg in 24 h and at 1000 mg/kg in 120 h treatments (Fig. 2B). These data indicate that *Vp*LAE and n-BF can promote oxidative stress in hepatocytes, with *Vp*LAE causing fewer changes in biochemical parameters than n-BF.

3.2. Biochemical analysis of the co-treatment regimen of Vernonanthura polyanthes leaf aqueous extract (VpLAE) or its n-butanol fraction (n-BF) with doxorubicin (DXR)

When *Vp*LAE was co-treated with DXR, SOD activity increased at 1000 mg/kg compared to the SOD activity in the group exposed to DXR alone (positive control). Meanwhile, CAT (at all concentrations) and GST (at 1000 mg/kg) had decreased activity (Fig. 3).

When n-BF was co-treated with DXR, SOD activity increased at all doses (250, 500, and 1000 mg/kg) compared with the SOD activity in the group exposed to DXR alone (positive control). Additionally, all doses significantly reduced MDA levels compared to the positive control (DXR alone), suggesting that n-BF effectively reduced DXR-induced oxidative damage (Fig. 4).

3.3. Biochemical analysis of the pre-treatment regimen of Vernonanthura polyanthes leaf aqueous extract (VpLAE) or its n-butanol fraction (n-BF) with doxorubicin (DXR)

In the pre-treatment, *Vp*LAE reduced lipid peroxidation levels (MDA), especially at lower doses (250 and 500 mg/kg), indicating a protective effect of the pre-treatment with *Vp*LAE against the damage caused by DXR (Fig. 3).

In the pre-treatment, n-BF increased SOD activity (at all doses) and GPx activity (at 250 mg/kg). MDA levels were reduced at 500 mg/kg, suggesting that intermediate doses of n-BF are effective in mitigating DXR-induced lipid peroxidation (Fig. 4). This suggests a non-linear dose-

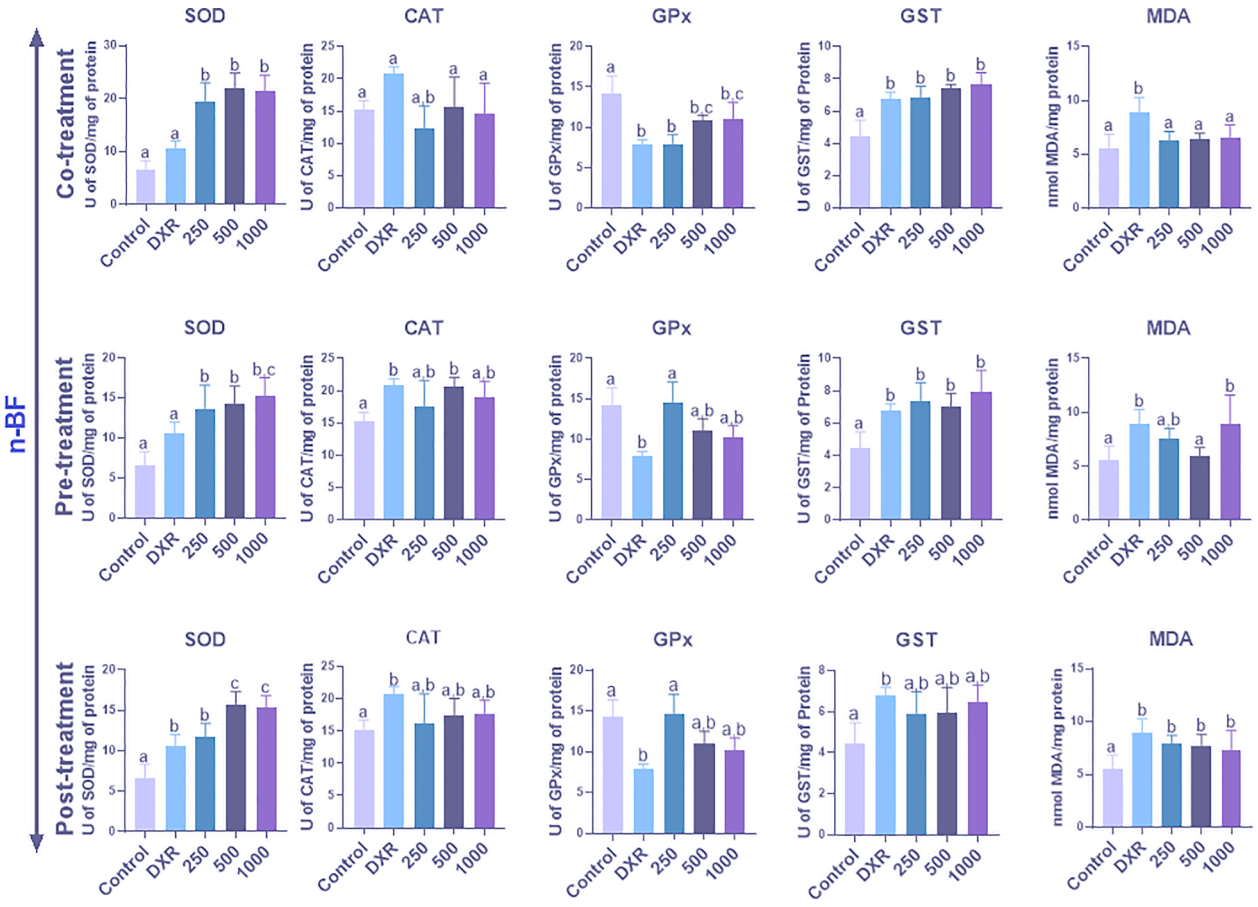

Fig. 4. Biochemical changes in the liver of mice treated with different doses (250, 500, and 1000 mg/kg) of the n-butanol fraction (n-BF) from the aqueous extract of the leaves of *Vernonanthura polyanthes* associated with doxorubicin (DXR) in several different treatments. Control: negative control (mineral water) and DXR: positive control (doxorubicin 15 mg/kg ip). The results are expressed as mean ± standard deviation. The groups were compared by ANOVA followed by Tukey's test (n = 5 animals per group). Different letters indicate statistically significant differences between groups ($p < 0.05$). The abbreviations SOD, CAT, GST, GPX and MDA mean superoxide dismutase, catalase, glutathione S-transferase, glutathione peroxidase, and malondialdehyde, respectively.

response relationship, consistent with a hormetic pattern.

3.4. Biochemical analysis of the post-treatment regimen of Vernonanthura polyanthes leaf aqueous extract (VpLAE) or its n-butanol fraction (n-BF) with doxorubicin (DXR)

In the post-treatment with *Vp*LAE, CAT had decreased activity at 500 and 1000 mg/kg; and GPx had increased activity at 1000 mg/kg (Fig. 3).

In the post-treatment, n-BF also increased SOD (at 500 and 1000 mg/kg) and GPx (at 250 mg/kg) activities. However, MDA levels were equal to those presented by DXR alone (Fig. 4).

3.5. 4-hydroxy-2-nonenal (4HNE) immunohistochemistry

The labeling decrease of 4HNE, an important marker of lipid peroxidation, in the liver of mice treated with DXR and *Vp*LAE or n-BF (Figs. 5–7) confirmed that the pre-treatment with *Vp*LAE (Fig. 5) and the co- (Fig. 6) and pre-treatments (Fig. 7) with n-BF reduced DXR-induced lipid peroxidation. Immunolabeling in the DXR groups (Figs. 5a, 6a, and 7a) showed a stronger peroxidase reaction, as indicated by the darker brown staining and confirmed by optical density quantification (Figs. 5d, 6d, and 7d). However, this parameter decreased in the groups supplemented with *Vp*LAE or n-BF (Figs. 5b,c, 6b,c, and 7b,c). As expected, 4HNE immunolabeling was correlated with the reduced levels of lipid peroxidation (MDA) observed in these *Vp*LAE- or n-BF-treated groups.

4. Discussion

Several strategies can help reduce oxidative stress caused by DRX, including the use of natural antioxidants (silymarin, naringin, resveratrol, and curcumin). These approaches can reduce not only oxidative stress but also inflammation and apoptosis (Zobeydi et al., 2025). *V. polyanthes* is being investigated as a possible chemotherapy adjuvant to overcome DXR side effects (Rocha et al., 2022). Previous phytochemical studies of *V. polyanthes* have identified several secondary metabolites, including polyphenols (flavonoids and phenolic acids), saponins, triterpenes, and sesquiterpene lactones (Bohlmann et al., 1981; Gallon et al., 2018; Igual et al., 2013; Rocha et al., 2022).

Polyphenols are a heterogeneous group of secondary metabolites that have in common the presence in their structure of one or more phenol groups. They can be divided into flavonoids and non-flavonoids, such as phenolic acids. Polyphenols can act as antioxidants or pro-oxidants, depending on concentration, structure, and the cellular environment, such as pH and the balance of redox-active transition metals (Dzah et al., 2024; León-González et al., 2015).

In this sense, first, the toxicity of *Vp*LAE and n-BF alone was investigated on the mouse liver tissue. Although only isolated increases in the analyzed antioxidant enzymes were observed, *Vp*LAE at the highest dose tested (1000 mg/kg) or n-BF at all tested doses increased oxidative stress in the livers of mice in a non-linear manner. *Vp*LAE also exhibited a toxic effect on *Artemia salina* and *Allium cepa* (Almeida et al., 2021; Kachena and Shackleton, 2024). For *A. cepa*, extract concentrations above 20 mg/mL were toxic to root cells, and cell division decreased at 40 mg/mL

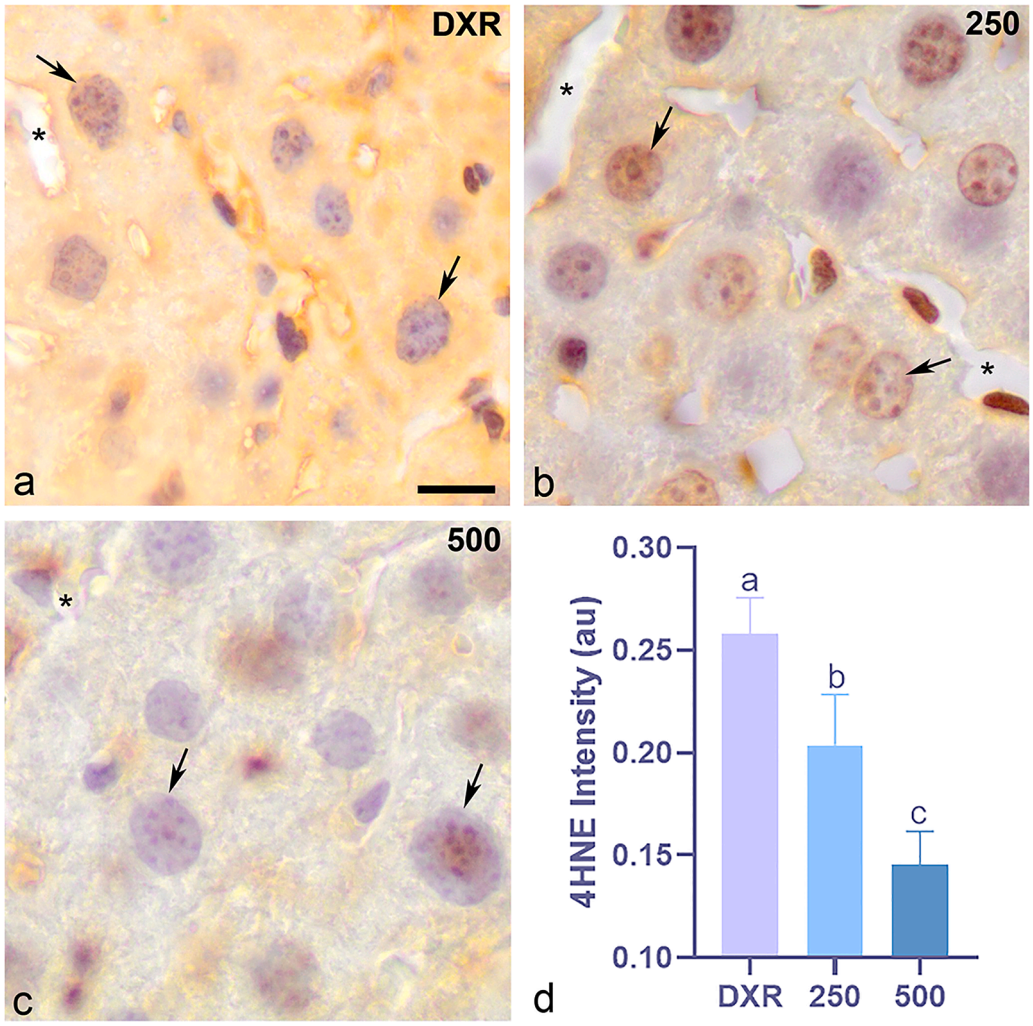

Fig. 5. Immunohistochemical staining and optical density (OD) quantification of 4-hydroxynonenal (4HNE) in liver tissue of mice pre-treated with the *Vernonanthura polyanthes* leaf aqueous extract (*Vp*LAE) and, after, doxorubicin (DXR). Representative photomicrographs of 4-hydroxynonenal (4HNE) immunostaining visualized with DAB and counterstained with hematoxylin from (a) liver tissues treated with DXR; (b) liver tissues pre-treated with 250 mg/kg *Vp*LAE; and (c) liver tissues pre-treated with 500 mg/kg *Vp*LAE. (d) optical density (mean gray value) obtained by color deconvolution analysis. The bars in the optical density graph (d) represent the mean ± SD (n = 6). Statistical significance ($p \leq 0.05$) was determined by one-way ANOVA and Tukey's post hoc test. There is no statistical difference between bars labeled with the same letter on the graphic. The scale bar corresponds to 10 μm and is the same for all figures. Arrows indicate hepatocyte nuclei, and asterisks indicate sinusoids. Brown marking shows a 4HNE-positive event. (au) stands for arbitrary units.

*Vp*LAE. For *A. salina*, 24 mg/mL *Vp*LAE killed 50% of the nauplii (Almeida et al., 2021). Similarly, the cytotoxicity of *V. polyanthes* leaf hydroalcoholic and alcoholic extracts has been previously demonstrated against mouse bone marrow erythrocytes (≥ 1000 mg/kg) (Jorgetto et al., 2011) and human lymphocytes (IC_{50} = 46.42 ± 3.50 μg/mL) (Feleti et al., 2020), respectively.

The cytotoxic effects of *V. polyanthes* may be related to the presence of polyphenols and their pro-oxidant mechanisms, such as (*i*) chemical instability; (*ii*) cellular glutathione depletion; (*iii*) autoxidation; (*iv*) generation of cytotoxic semiquinone radical; (*v*) direct generation of ROS; and (*vi*) reduction of metal ions involved in redox-cycling and generation of hydroxyl radicals through Fenton and Fenton-like reactions, in higher doses/concentrations (Jain et al., 2025; León-González et al., 2015). Flavonoid prooxidant properties seem to be concentration-dependent (Procházková et al., 2011). However, the pro-oxidant potential of polyphenols does not diminish their health benefits, especially at physiologically relevant concentrations (Jain et al., 2025). The potential of polyphenols at low doses to induce a mild oxidative stress response in normal cells, thereby activating endogenous antioxidant systems and other protective mechanisms (i.e., adaptive responses), is known as hormesis and can result in a cytoprotective effect (Jain et al., 2025).

When mice were treated with DXR, administration of *Vp*LAE or n-BF caused little variation in the antioxidant enzymes analyzed, particularly CAT, SOD, and GPx. However, *Vp*LAE or n-BF reduced MDA levels, a product of lipid peroxidation, especially the pre-treatment with *Vp*LAE (250 and 500 mg/kg) and co- (500 and 1000 mg/kg) and pre-treatments (250 and 500 mg/kg) with n-BF. These data were corroborated by a decrease in 4HNE labeling, another important marker of lipid peroxidation (Ayala et al., 2014). Lipid peroxidation is a process in which oxidants, such as free radicals, can initiate the oxidative decomposition of cell membranes. In this process, a wide variety of reactive aldehydes are produced intracellularly, including MDA and 4HNE (Ayala et al., 2014). In this context, the TBARS assay, which measures MDA, can be used in combination with other lipid peroxidation indices, such as 4HNE immunohistochemical labeling, to assess oxidative stress status in a tissue (Endale et al., 2023; Grotto et al., 2009).

As antioxidants, polyphenols can function through different pathways, such as (*i*) scavenging oxidants (sharing lone-pair electrons to complex other pro-oxidants and/ or transition metals or donating their hydrogen atoms to free radicals, such as ROS); (*ii*) chelating metals that promote oxidative stress; and/or (*iii*) inducing the expression of genes

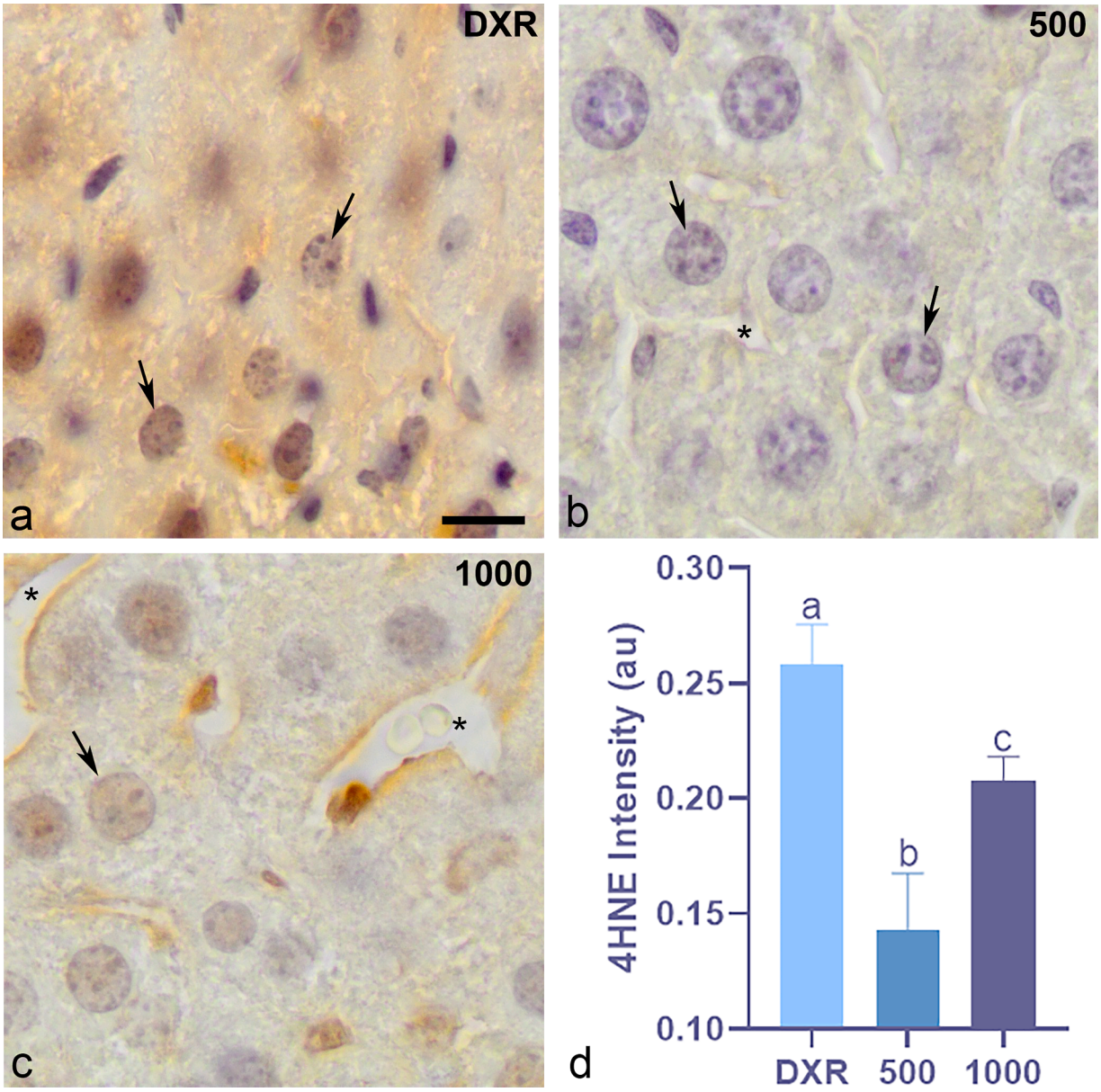

Fig. 6. Immunohistochemical staining and optical density (OD) value of 4-hydroxynonenal (4HNE) in liver tissue of mice co-treated with the n-butanol fraction (n-BF) of the *Vernonanthura polyanthes* leaf aqueous extract and doxorubicin (DXR). Representative photomicrographs of 4-hydroxynonenal (4HNE) immunostaining visualized with DAB and counterstained with hematoxylin from (a) liver tissues treated with DXR; (b) liver tissues treated with 500 mg/kg n-BF and DXR; and (c) liver tissues treated with 1000 mg/kg n-BF and DXR. (d) optical density (mean gray value) obtained by color deconvolution analysis. The bars in the optical density graph (d) represent the mean ± SD (n = 6). Statistical significance ($p \leq 0.05$) was determined by one-way ANOVA and Tukey's post hoc test. There is no statistical difference between bars labeled with the same letter on the graphic. The scale bar corresponds to 10 μm and is the same for all figures. Arrows indicate hepatocyte nuclei, and asterisks indicate sinusoids. Brown marking shows a 4HNE-positive event. (au) stands for arbitrary units.

encoding detoxifying enzymes (Bolaños-Cardet et al., 2026; Dai and Mumper, 2010; Dzah et al., 2024). In this way, the co-administration of polyphenols with conventional cancer chemotherapic drugs, such as DXR, which disrupts normal cellular iron metabolism (Ye et al., 2024), has been proposed as a promising strategy in order to increase selectivity against cancer cells, to reduce drug resistance, and to prevent the deleterious effects of the anticancer therapy on normal cells (Pratheeshkumar et al., 2012).

The hepatoprotective potential of *V. polyanthes* against DXR-induced oxidative stress corroborates previous data showing that *Vp*LAE and n-BF exhibited high cytoprotective potential against the toxic effects of DXR (Rocha et al., 2022). This cytoprotective activity may be correlated with the antioxidant potential of the phenolic compounds present in *Vp*LAE and n-BF (Igual et al., 2013; Rocha et al., 2022; Rodrigues and Carvalho, 2001). *V. polyanthes* also demonstrated antigenotoxic properties, maybe due to the presence of compounds with antioxidant properties that impair DNA damage (Rocha et al., 2022).

According to computational data prediction, the metabolites identified in *Vp*LAE and n-BF exhibited antioxidant and chemoprotective potential, with rutin, a glycosylated quercetin, being particularly noteworthy (Aguiar et al., 2024; Rocha et al., 2022). Rutin can directly eliminate ROS, playing a fundamental role in reducing oxidative stress (Pravin et al., 2024). A series of studies have demonstrated its high antioxidant potential, which triggers an increase in the activity of antioxidant enzymes such as GST, CAT, GPx, SOD, and GR (Glutathione Reductase), increasing GSH (Glutathione) content and reducing MDA (Li et al., 2022), similar to what was observed in this work. Rutin attenuated the toxic effects of DXR in cardiac and renal tissues by enhancing the

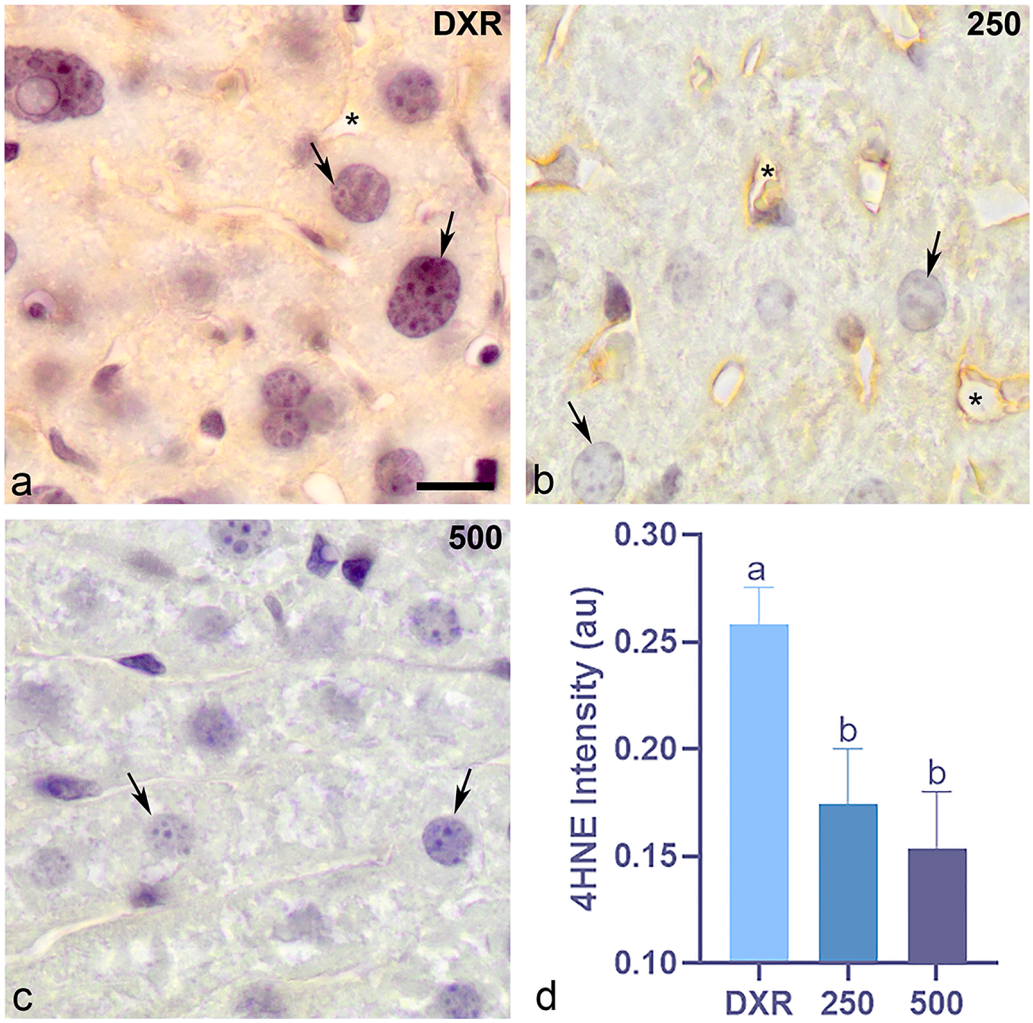

Fig. 7. Immunohistochemical staining and optical density (OD) value of 4-hydroxynonenal (4HNE) in liver tissue of mice pre-treated with the n-butanol fraction (n-BF) of the *Vernonanthura polyanthes* leaf aqueous extract and, after, doxorubicin (DXR). Representative photomicrographs of 4-hydroxynonenal (4HNE) immunostaining visualized with DAB and counterstained with hematoxylin from (a) liver tissues treated with DXR; (b) liver tissues pre-treated with 250 mg/kg n-BF; and (c) liver tissues pre-treated with 500 mg/kg n-BF. (d) optical density (mean gray value) obtained by color deconvolution analysis. The bars in the optical density graph (d) represent the mean ± SD (n = 6). Statistical significance ($p \leq 0.05$) was determined by one-way ANOVA and Tukey's post hoc test. There is no statistical difference between bars labeled with the same letter on the graphic. The scale bar corresponds to 10 μm and is the same for all figures. Arrows indicate hepatocyte nuclei, and asterisks indicate sinusoids. Brown marking shows a 4HNE-positive event. (au) stands for arbitrary units.

cellular antioxidant status (Mahmoud et al., 2020; Rocha et al., 2022). Rutin and its aglycone, quercetin, are capable of suppressing free radical processes in three stages: the formation of superoxide ions, the generation of hydroxyl radicals, and the Fenton reaction, since they are able to chelate and oxidize transition metal ions (Afanas'ev et al., 1989; Dzah et al., 2024).

However, rutin and quercetin tested over a wide range of concentrations (50 - 4000 mol/L) exhibited dual pro-oxidant and antioxidant activity, consisting of the enhancement or suppression of MDA formation, respectively (Fukumoto and Mazza, 2000). Quercetin in the range of 25–200 μM increased H_2O_2, superoxide anion radical, and TBARS in a linear behavior in human lymphocytes (Yen et al., 2003). Similarly, quercetin at 100 μM increased oxidative DNA damage in human leucocytes (Wilms et al., 2008). These results were supported by electron spin resonance findings for quercetin in solution, which also showed a pro-oxidant effect at 100 μM (Wilms et al., 2008). Quercetin at 100 μM also greatly enhanced hydroxyl radical formation up to eight-fold in rat liver microsomes (Laughton et al., 1989). In contrast, quercetin inhibited iron-induced lipid peroxidation in rat liver microsomes (Laughton et al., 1989) and reduced oxidative DNA damage in human leucocytes (Wilms et al., 2008) at low micromolar concentrations (≤1.5 μM and 1–50 μM, respectively). However, it is important to note that quercetin and rutin do not exhibit the same behavior in all situations, suggesting that structural modification also alters the pro-oxidant pattern (Procházková et al., 2011).

The relationship between the structure of rutin, quercetin, and its methyl ethyl and hydroxyl-ethyl derivatives and their scavenging activity against superoxide, hydroxyl, and peroxyl radicals was studied (Kessler et al., 2003). Alkylation of the hydroxyl at position 7 increased free radical scavenging. On the other hand, some rutin derivatives with a free catechol moiety or a free hydroxyl group at position 3 (or both) were pro-oxidants, producing superoxide radicals and hydrogen peroxide. It appears that, to prevent pro-oxidant behavior, the hydroxyl group at position 3 must be blocked to avoid its auto-oxidation (Kessler et al., 2003).

A similar behavior was observed for chlorogenic acids, also detected in *Vp*LAE and n-BF (Rocha et al., 2022). They can shift their activity from pro-oxidant to antioxidant (or vice versa) as the concentration increases from 5 to 50 mol/L. This dual behavior could be explained by the presence of catechol or methoxyphenol in the backbone structures of phenolics, which efficiently scavenge $^{\bullet}OH$ radicals (antioxidant activity) and regenerate Fe^{2+} by the reduction of Fe^{3+} (pro-oxidant activity)

(Nowak et al., 2022).

This ambivalent character of polyphenols, which can act simultaneously as antioxidants and pro-oxidants (Andrés et al., 2023), may explain the toxicity observed by *Vp*LAE and n-BF on the mouse liver in higher doses; and their hepatoprotective potential of *V. polyanthes* against DXR-induced oxidative stress. Therefore, evaluating the overall antioxidant capacity of polyphenols requires considering the interplay of diverse factors, along with the specific cellular context (Jain et al., 2025). Additionally, numerous points still remain to be clarified in this polyphenol-rich extracts as adjuvants in cancer therapy strategy, such as (*i*) the bioavailability of polyphenols, affected by the interaction with other dietary components and the gut microbiota (Hussain et al., 2016); (*ii*) the polyphenols pharmocodynamics, such as absorption, metabolism, distribution, and excretion within the body (Jain et al., 2025); (*iii*) the best concentration and molecular structure of the active polyphenols; (*iv*) the role of polyphenolic metabolites; (*v*) the clinical evidence of their therapeutic potential (León-González et al., 2015); (*vi*) and the administration regimen (pre-, co-, or post-treatment). Understanding these complex tasks involving the pharmacological use of polyphenols will allow the design of specific therapies that can serve science and medicine (Andrés et al., 2023).

5. Conclusion

*Vp*LAE at 250 and 500 mg/kg and n-BF at 1000 mg/kg did not increase MDA levels in the livers of mice. The pre-treatment with *Vp*LAE (250 and 500 mg/kg), and the co- (500 and 1000 mg/kg) and pre-treatments (250 and 500 mg/kg) with n-BF reduced MDA levels and 4HNE labeling in the livers of mice also treated with DXR, indicating a reduction in lipid peroxidation promoted by DXR. Based on the gathered data, these treatment regimens could confer a protective effect against oxidative damage caused by DXR in mice livers. However, the data obtained at this moment are exploratory and require further complementary studies. The biochemical data did not show a dose-response relationship and revealed dual effects in the presence and absence of DXR, reinforcing the ambivalent character of polyphenols, which can act as both antioxidants and pro-oxidants. Moreover, these analyses should be extended to cancer cell lines to test the hypothesis that *Vp*LAE or n-BF could be promising candidates for counteracting DXR side effects.

Funding

This research was funded by Fundação de Amparo à Pesquisa do Estado de Goiás (FAPEG; grant numbers PPP/201610267001019 and Bioprospecta Cerrado/202510267001859). JDR was supported by a scholarship from Conselho Nacional de Desenvolvimento Científico e Tecnológico (CNPq), and EFLCB is granted with a productivity fellowship from FAPEG (proc. 202510267001605).

Data availability statement

Data available on request from the authors.

CRediT authorship contribution statement

Jamira Dias Rocha: Writing – original draft, Formal analysis, Conceptualization. **Lara Lorhany Gomes da Costa Rodrigues:** Formal analysis. **Hericles Mesquita Campos:** Writing – original draft, Formal analysis. **Robbert Mota Pereira:** Formal analysis. **Abel Vieira de Melo Bisneto:** Writing – original draft, Formal analysis. **Samantha Salomão Caramori:** Writing – review & editing, Methodology. **Lee Chen-Chen:** Writing – review & editing, Methodology, Investigation. **Paulo César Ghedini:** Writing – review & editing, Methodology, Funding acquisition. **Manoel Francisco Biancardi:** Writing – review & editing, Writing – original draft, Methodology, Investigation. **Elisa Flávia Luiz Cardoso Bailão:** Writing – review & editing, Supervision, Project administration, Funding acquisition, Conceptualization.

Declaration of interest statement

The authors declare that they have no known competing financial interests or personal relationships that could have appeared to influence the work reported in this paper.

Acknowledgements

Not applicable.

Supplementary materials

Supplementary material associated with this article can be found, in the online version, at doi:10.1016/j.sajb.2026.04.014.

References

Abbas, N.A.T., Awad, M.M., Nafea, E., 2021. Silymarin in combination with chlorogenic acid protects against hepatotoxicity induced by doxorubicin in rats: possible role of adenosine monophosphate-activated protein kinase pathway. Toxicol. Res. 9, 771–777. https://doi.org/10.1093/TOXRES/TFAA080.

Afanas'ev, I.B., Dcrozhko, A.I., Brodskii, A.V., Kostyuk, V.A., Potapovitch, A.I., 1989. Chelating and free radical scavenging mechanisms of inhibitory action of rutin and quercetin in lipid peroxidation. Biochem. Pharmacol. 38, 1763–1769. https://doi.org/10.1016/0006-2952(89)90410-3.

Aguiar, A.S.N.d., Rodrigues, L.L.G.d.C., Rocha, J.D., Guimarães, L.M.M., Ramos, L.C.C., Napolitano, H.B., Bailão, E.F.L.C., Borges, A.L.L., 2024. Theoretical exploration of the antioxidant activity, chemopreventive, and antineoplastic potentials of molecules present in *Morinda lucida, Momordica charantia*, and *Vernonanthura polyanthes*. J. Comput. Biophys. Chem. 23. https://doi.org/10.1142/S2737416524500108.

Alherz, F.A., Negm, W.A., El-Masry, T.A., Elmorshedy, K.E., El-Kadem, A.H., 2023. The potential beneficial role of Ginkgetin in doxorubicin-induced hepatotoxicity: elucidating the underlying claim. Biomed. Pharmacother. 165, 1–13. https://doi.org/10.1016/j.biopha.2023.115010.

Almeida, L.M., Prado, A.D.L., Xavier-Silva, K.R., Firmino, M.T., Paula, M.I.M., Gomes, P. N., Paula, J.A.M., Bailão, E.F.L.C., 2021. Cytotoxic effect of *Vernonanthura polyanthes* leaves aqueous extracts. Braz. J. Biol. 81, 575–583. https://doi.org/10.1590/1519-6984.225281.

Andrés, C.M.C., Pérez de la Lastra, J.M., Juan, C.A., Plou, F.J., Pérez-Lebeña, E., 2023. Polyphenols as antioxidant/pro-oxidant compounds and donors of reducing species: relationship with human antioxidant metabolism. Processes 11, 1–23. https://doi.org/10.3390/pr11092771.

Ayala, A., Muñoz, M.F., Argüelles, S., 2014. Lipid peroxidation: production, metabolism, and signaling mechanisms of malondialdehyde and 4-hydroxy-2-nonenal. Oxid. Med. Cell. Longev. 1–31. https://doi.org/10.1155/2014/360438.

Bohlmann, F., Jakupovic, J., Gupta, R.K., Kingt, R.M., Berlin, D., Germany, W., 1981. Allenic germacranolides, bourbonene derived lactones and other constituents from Vernonia species. Phytochemistry 20, 473–480. https://doi.org/10.1016/S0031-9422(00)84169-2.

Bolaños-Cardet, J., Pepió-Tárrega, B., Saiz-Poseu, J., López-Moral, A., Ullah, F., Yuste, V. J., Ruiz-Molina, D., Suárez-García, S., 2026. The redox properties of polyphenols and their role in ROS generation for biomedical applications. Angew. Chem. - Int. Ed. 65, 1–40. https://doi.org/10.1002/anie.202513698.

Bradford, M.M., 1976. A rapid and sensitive method for the quantification of microgram quantities of protein utilizing the principle of protein-dye-binding. Anal Biochem. 72, 248–254. https://doi.org/10.1016/0003-2697(76)90527-3.

Brasil, 2011. Formulário De Fitoterápicos da Farmacopeia Brasileira. Agência Nacional de Vigilância Sanitária.

Camaggi, C.M., Comparsi, R., Strocchi, E., Testoni, F., Angelelli, B., Pannuti, F., 1988. Epirubicin and doxorubicin comparative metabolism and pharmacokinetics - a cross-over study. Cancer Chemother. Pharmacol. 21, 221–228. https://doi.org/10.1007/BF00262774.

Campos, H.M., Pereira, R.M., de Oliveira Ferreira, P.Y., Uchenna, N., Branco da Silva, C. R., Pruccoli, L., Sanz, G., Rodrigues, M.F., Vaz, B.G., Rivello, B.G., Batista da Rocha, A.L., de Carvalho, F.S., Oliveira, G.d.A.R., Lião, L.M., Georg, R., de, C., Leite, J.A., dos Santos, F.C.A., Costa, E.A., Menegatti, R., Tarozzi, A., Ghedini, P.C., 2024. A novel arylpiperazine derivative (LQFM181) protects against neurotoxicity induced by 3- nitropropionic acid in in vitro and in vivo models. Chem. Biol. Interact. 395, 111026. https://doi.org/10.1016/j.cbi.2024.111026.

Chaves, T.L., Ricardo, L., de Paula-Souza, J., Brandão, M.d.G.L., 2015. Useful Brazilian plants under the view of the writer-naturalist João Guimarães Rosa. Rev. Bras. Farmacogn. 25, 437–444. https://doi.org/10.1016/j.bjp.2015.06.003.

Cheng, Y., Wu, X., Nie, X., Wu, Y., Zhang, C., Lee, S.M.Y., Lv, K., Leung, G.P.H., Fu, C., Zhang, J., Li, J., 2022. Natural compound glycyrrhetinic acid protects against doxorubicin-induced cardiotoxicity by activating the Nrf2/HO-1 signaling pathway. Phytomedicine 106, 154407. https://doi.org/10.1016/j.phymed.2022.154407.

Dai, J., Mumper, R.J., 2010. Plant phenolics: extraction, analysis and their antioxidant and anticancer properties. Molecules 15, 7313–7352. https://doi.org/10.3390/molecules15107313.

Damodar, G., Smitha, T., Gopinath, S., Vijayakumar, S., Rao, Y., 2014. An evaluation of hepatotoxicity in breast cancer patients receiving injection doxorubicin. Ann. Med. Health Sci. Res. 4, 74–79. https://doi.org/10.4103/2141-9248.126619.

Dzah, C.S., Zhang, H., Gobe, V., Asante-Donyinah, D., Duan, Y., 2024. Anti- and pro-oxidant properties of polyphenols and their role in modulating glutathione synthesis, activity and cellular redox potential: potential synergies for disease management. Adv. Redox Res. 11, 1–11. https://doi.org/10.1016/j.arres.2024.100099.

Endale, H.T., Tesfaye, W., Mengstie, T.A., 2023. ROS induced lipid peroxidationand their role in ferroptosis. Cell Dev. Biol. 11, 1. https://doi.org/10.3389/fcell.2023.1226044.

Feleti, S.M.V., Aleluia, R.L., Gervásio, S.V., Dutra, J.C.V., Oliveira, R.P., Rita de Cássia R, J., Gonçalves, R.d., Jamal, C.M., Kuster, R.M., Brasileiro, B.G., Batitucci, M.d.C.P., 2020. Phytochemical screening, antioxidant, anti-cytotoxic and anticancer effects of *Galinsoga parviflora* and *Vernonia polyanthes* (asteraceae) extracts. Int. J. Res. -Granthaalayah 8, 84–98. https://doi.org/10.29121/granthaalayah.v8.i10.2020.1782.

Forrest, R.A., Swift, L.P., Rephaeli, A., Nudelman, A., Kimura, K.I., Phillips, D.R., Cutts, S. M., 2012. Activation of DNA damage response pathways as a consequence of anthracycline-DNA adduct formation. Biochem. Pharmacol. 83, 1602–1612. https://doi.org/10.1016/j.bcp.2012.02.026.

Fukumoto, L.R., Mazza, G., 2000. Assessing antioxidant and prooxidant activities of phenolic compounds. J. Agric. Food Chem. 48, 3597–3604. https://doi.org/10.1021/jf000220w.

Gallon, M.E., Monge, M., Casoti, R., Da Costa, F.B., Semir, J., Gobbo-Neto, L., 2018. Metabolomic analysis applied to chemosystematics and evolution of megadiverse Brazilian Vernonieae (Asteraceae). Phytochemistry 150, 93–105. https://doi.org/10.1016/j.phytochem.2018.03.007.

Grotto, D., Santa Maria, L., Valentini, J., Paniz, C., Schimitt, G., Garcia, S.C., Pomblum, V.J., Rocha, J.B.T., Farina, M., 2009. Importance of the lIpId peroxIdatIon bIomarkers and methodologIcal aspects for malondIaldehyde quantIfIcatIon. Quim. Nova 32, 169–174. https://doi.org/10.1590/S0100-40422009000100032.

Guo, J., Guo, Q., Fang, H., Lei, L., Zhang, T., Zhao, J., Peng, S., 2014. Cardioprotection against doxorubicin by metallothionein is associated with preservation of mitochondrial biogenesis involving PGC-1α pathway. Eur. J. Pharmacol. 737, 117–124. https://doi.org/10.1016/j.ejphar.2014.05.017.

Halil, I., Disli, F., Bayindir, S., Toprak, M., Riza, A., Sahin, A., Altun, M., Kocak, A., Demirtas, I., Adem, S., 2021. The isolation of secondary metabolites from *Rheum ribes* L . and the synthesis of new semi-synthetic anthraquinones : isolation, synthesis and biological activity. Food Chem. 342, 128378. https://doi.org/10.1016/j.foodchem.2020.128378.

Husna, F., Arozal, W., Yusuf, H., Safarianti, S., 2022. Protective effect of mangiferin on doxorubicin-induced liver damage in animal model. J. Res. Pharm. 26 (1), 44–51.

Hussain, S.M., Hussain, M.S., Ahmed, A., Arif, N., 2016. Characterization of isolated bioactive phytoconstituents from *Flacourtia indica* as potential phytopharmaceuticals, an in silico perspective 5, 323–331.

Igual, M.O., Martucci, M.E.P., Da Costa, F.B., Gobbo-Neto, L., 2013. Sesquiterpene lactones, chlorogenic acids and flavonoids from leaves of *Vernonia polyanthes* less (Asteraceae). Biochem. Syst. Ecol. 51, 94–97. https://doi.org/10.1016/j.bse.2013.08.018.

Jain, P.K., Parashar, A.K., Shrivastava, V., 2025. A review on exploring the health benefits and antioxidant properties of bioactive polyphenols. Discov. Food 5, 1–18. https://doi.org/10.1007/s44187-025-00637-7.

Jorgetto, G.V., Boriolo, M.F.G., Silva, L.M., Nogueira, D.A., José, T.D.d.S., Ribeiro, G.E., Oliveira, N.d.M.S., Fiorini, J.E., 2011. Ensaios de atividade antimicrobiana in vitro e mutagênica in vivo com extrato de *Vernonia polyanthes* less (Assa-peixe). Rev. Inst. Adolfo Lutz 70, 53–61.

Kachena, L., Shackleton, R.T., 2024. The impact of the invasive alien plant *Vernonanthura polyanthes* on conservation and livelihoods in the Chimanimani uplands of Zimbabwe. Biol. Invasions 26, 1749–1767. https://doi.org/10.1007/s10530-024-03275-9.

Kato, S., Naito, Z., 1999. Glutathione S-transferase. Nippon rinsho. Jpn. J. Clin. Med. 57 (22), 451–453.

Kessler, M., Ubeaud, G., Jung, L., 2003. Anti- and pro-oxidant activity of rutin and quercetin derivatives. J. Pharm. Pharmacol. 55, 131–142. https://doi.org/10.1211/002235702559.

Laughton, M.J., Halliwell, B., Evans, P.J., Robin, J., Hoult, S., 1989. Antioxidant and pro-oxidant actions of the plant phenolics quercetin, gossypol and myricetin. Effects on lipid peroxidation, hydroxyl radical generation and bleomycin-dependent damage to DNA. Biochem. Pharmacol. 38, 2859–2865. https://doi.org/10.1016/0006-2952(89)90442-5.

León-González, A.J., Auger, C., Schini-Kerth, V.B., 2015. Pro-oxidant activity of polyphenols and its implication on cancer chemoprevention and chemotherapy. Biochem. Pharmacol. 98, 371–380. https://doi.org/10.1016/j.bcp.2015.07.017.

Li, N., Liu, J., Yang, L., Kang, Y., Cao, Y., Chen, K., Sun, H., Chen, W., Dai, Q., Sakai, Y., 2022. Synergistic effect of antioxidant systems enhance cadmium phytoextraction and translocation in Amaranthus hypochondriacus under rutin application. S. Afr. J. Bot. 149, 582–590. https://doi.org/10.1016/j.sajb.2022.06.053.

Lorenzi, H., Matos, F.J.A., 2002. Plantas Medicinais no Brasil: Nativas e Exóticas. Instituto Plantarum, Nova Odessa.

Mahmoud, H.U.R., Ahmed, O.M., Fahim, H.I., Ahmed, N.A., Ashour, M.B., 2020. Effects of rutin and quercetin on doxorubicin-induced renocardiotoxicity in male wistar rats. Adv. Anim. Vet. Sci. 8, 370–384. https://doi.org/10.17582/JOURNAL.AAVS/2020/8.4.370.384.

Mahmoudi, F., Arasteh, O., Elyasi, S., 2023. Preventive and therapeutic use of herbal compounds against doxorubicin induced hepatotoxicity: a comprehensive review. Naunyn-Schmiedeb. Arch. Pharmacol. 396, 1595–1617. https://doi.org/10.1007/s00210-023-02429-1.

Nowak, M., Tryniszewski, W., Sarniak, A., Wlodarczyk, A., Nowak, P.J., Nowak, D., 2022. Concentration dependence of anti- and pro-oxidant activity of polyphenols as evaluated with a light-emitting Fe2+-egta-H2O2 system. Molecules 27, 1–17. https://doi.org/10.3390/molecules27113453.

Octavia, Y., Tocchetti, C.G., Gabrielson, K.L., Janssens, S., Crijns, H.J., Moens, A.L., 2012. Doxorubicin-induced cardiomyopathy: from molecular mechanisms to therapeutic strategies. J. Mol. Cell. Cardiol. 52, 1213–1225. https://doi.org/10.1016/j.yjmcc.2012.03.006.

OECD, 2001. Test No. 423: acute oral toxicity - acute toxic class method, OECD Guidelines for the testing of chemicals. OECD Guidel. Test. Chem. 4, 1–14.

OECD, 2016. Oecd 474: Guideline for the Testing of Chemicals: Mammalian Erythrocyte Micronucleus Test. Oecd Guideline For The Testing of Chemicals, 474.

Okoh, V.I., Campos, H.M., de Oliveira Ferreira, P.Y., Pereira, R.M., Silva, Y.S., Arruda, E. L., Pagliarani, B., de Almeida Ribeiro Oliveira, G., Lião, L.M., dos Santos, G.F., Vaz, B.G., Sabino, J.R., dos Santos, F.C.A., Costa, E.A., Tarozzi, A., Menegatti, R., Ghedini, P.C., 2024. Chrysin bonded to β-d-glucose tetraacetate enhance its protective effects against the neurotoxicity induced by aluminum in Swiss mice. J. Pharm. Pharmacol. 76, 368–380. https://doi.org/10.1093/jpp/rgae011.

Prasanna, P.L., Renu, K., Valsala Gopalakrishnan, A., 2020. New molecular and biochemical insights of doxorubicin-induced hepatotoxicity. Life Sci. 250, 117599. https://doi.org/10.1016/j.lfs.2020.117599.

Pratheeshkumar, P., Sreekala, C., Zhang, Z., Budhraja, A., Songze, D., Son, Y.-O., Wang, X., Hitron, A., Hyun-Jung, K., Wang, L., Lee, J.-C., Shi, X., 2012. Cancer prevention with promising natural products: mechanisms of action and molecular targets. Anticancer Agents Med. Chem. 12, 1–50.

Pravin, B., Nanaware, V., Ashwini, B., Wondmie, G.F., Jardan, Y.A.B., Bourhia, M., 2024. Assessing the antioxidantproperties of Naringin and Rutinand investigating their oxidativeDNA damage effects in breastcancer. Sci. Rep. 14, 1–20. https://doi.org/10.1038/s41598-024-63498-7.

Procházková, D., Boušová, I., Wilhelmová, N., 2011. Antioxidant and prooxidant properties of flavonoids. Fitoterapia 82, 513–523. https://doi.org/10.1016/j.fitote.2011.01.018.

Radeva, L., Yoncheva, K., 2025. Doxorubicin toxicity and recent approaches to alleviating its adverse effects with focus on oxidative stress. Molecules 30, 1–26. https://doi.org/10.3390/molecules30153311.

Rehman, M.U., Tahir, M., Khan, A.Q., Khan, R., Oday-O-Hamiza Lateef, A., Hassan, S.K., Rashid, S., Ali, N., Zeeshan, M., Sultana, S., 2014. d-limonene suppresses doxorubicin-induced oxidative stress and inflammation via repression of COX-2, iNOS, and NFκB in kidneys of Wistar rats. Exp. Biol. Med. 239, 465–476. https://doi.org/10.1177/1535370213520112.

Rocha, J.D., Ferreira, J.d.S., Silva, J.G.V., Fernandes, A.S., Véras, J.H., Almeida, L.M.d., Teles, A.M., Borges, L.L., Chen-Chen, L., Bailão, E.F.L.C., 2020. In vitro hematotoxicity of *Vernonanthura polyanthes* leaf aqueous extract and its fractions. Drug Chem. Toxicol. 0, 1–9. https://doi.org/10.1080/01480545.2020.1802481.

Rocha, J.D., Gallon, M.E., Bisneto, A.V.d.M., Amaral, V.C.S., de Almeida, L.M., Borges, L. L., Chen-Chen, L., Gobbo-Neto, L., Bailão, E.F.L.C., 2022. Phytochemical composition and protective effect of *Vernonanthura polyanthes* leaf against in vivo doxorubicin-mediated toxicity. Molecules 27. https://doi.org/10.3390/molecules27082553.

Rodrigues, V.E.G., Carvalho, D.A.D., 2001. Levantamento etnobotânico de plantas medicinais no domíniodo cerrado na região do alto etnobotanical survey of medicinal plants in the dominion of meadows in the region of the Alto Rio Grande - Minas Gerais. Ciênc. Agratecnologia 25, 102–123.

Samare-Najaf, M., Zal, F., Safari, S., 2020. Primary and secondary markers of doxorubicin-induced female infertility and the alleviative properties of quercetin and vitamin E in a rat model. Reprod. Toxicol. 96, 316–326. https://doi.org/10.1016/j.reprotox.2020.07.015.

Schindelin, J., Arganda-Carreras, I., Frise, E., Kaynig, V., Longair, M., Pietzsch, T., Preibisch, S., Rueden, C., Saalfeld, S., Schmid, B., Tinevez, J.Y., White, D.J., Hartenstein, V., Eliceiri, K., Tomancak, P., Cardona, A., 2012. Fiji: an open-source platform for biological-image analysis. Nat. Methods 9, 676–682. https://doi.org/10.1038/nmeth.2019.

Shivakumar, P., Usha Rani, M., Gopala Reddy, A., Anjaneyulu, Y., 2012. A study on the toxic effects of doxorubicin on the histology of certain organs. Toxicol. Int. 19, 241–244. https://doi.org/10.4103/0971-6580.103656.

Silva, C.A., Véras, J.H., Ventura, J.A., de Melo Bisneto, A.V., de Oliveira, M.G., Cardoso Bailão, E.F.L., e Silva, C.R., Cardoso, C.G., da Costa Santos, S., Chen-Chen, L., 2023. Chemopreventive effect and induction of DNA repair by oenothein B ellagitannin isolated from leaves of *Eugenia uniflora* in Swiss Webster treated mice. J. Toxicol. Environ. Health - A: Curr. Issues 86, 929–941. https://doi.org/10.1080/15287394.2023.2259425.

Singal, P.K., Iliskovic, N., 1998. Doxorubicin-induced Cardiomyopathy. The New England Journal of Medicine. https://doi.org/10.1056/NEJM199809243391307.

Singal, P.K., Li, T., Kumar, D., Danelisen, I., Iliskovic, N., 2000. Adriamycin-induced heart failure: mechanism and modulation. Mol. Cell. Biochem. 207, 77–86. https://doi.org/10.1023/a:1007094214460.

Songbo, M., Lang, H., Xinyong, C., Bin, X., Ping, Z., Liang, S., 2019. Oxidative stress injury in doxorubicin-induced cardiotoxicity. Toxicol. Lett. 307, 41–48. https://doi.org/10.1016/j.toxlet.2019.02.013.

Thorn, C.F., Oshiro, C., Marsh, S., Hernandez-Boussard, T., McLeod, H., Klein, T.E., Altman, R.B., 2011. Doxorubicin pathways: pharmacodynamics and adverse effects.

Pharmacogenet. Genom. 21, 440–446. https://doi.org/10.1097/FPC.0b013e32833ffb56.

Tribess, B., Pintarelli, G.M., Bini, L.A., Camargo, A., Funez, L.A., De Gasper, A.L., Zeni, A. L.B., 2015. Ethnobotanical study of plants used for therapeutic purposes in the Atlantic Forest region, Southern Brazil. J. Ethnopharmacol. 164, 136–146. https://doi.org/10.1016/j.jep.2015.02.005.

Wattanapitayakul, S.K., Chularojmontri, L., Herunsalee, A., Charuchongkolwongse, S., Niumsakul, S., Bauer, J.A., 2005. Screening of antioxidants from medicinal plants for cardioprotective effect against doxorubicin toxicity. Basic Clin. Pharmacol. Toxicol. 96, 80–87. https://doi.org/10.1111/j.1742-7843.2005.pto960112.x.

Wilms, L.C., Kleinjans, J.C.S., Moonen, E.J.C., Briedé, J.J., 2008. Discriminative protection against hydroxyl and superoxide anion radicals by quercetin in human leucocytes in vitro. Toxicol. Vitro 22, 301–307. https://doi.org/10.1016/j.tiv.2007.09.002.

Xu, M.F., Tang, P.L., Qian, Z.M., Ashraf, M., 2001. Effects by doxorubicin on the myocardium are mediated by oxygen free radicals. Life Sci. 68, 889–901. https://doi.org/10.1016/S0024-3205(00)00990-5.

Ye, H., Wu, L., Liu, Y., 2024. Iron metabolism in doxorubicin-induced cardiotoxicity: from mechanisms to therapies. Int. J. Biochem. Cell Biol. 174, 106–632. https://doi.org/10.1016/j.biocel.2024.106632.

Yen, G.C., Duh, P.D., Tsai, H.L., Huang, S.L., 2003. Pro-oxidative properties of flavonoids in human lymphocytes. Biosci. Biotechnol. Biochem. 67, 1215–1222. https://doi.org/10.1271/bbb.67.1215.

Zobeydi, A.M., Mousavi Namavar, S.N., Sadeghi Shahdani, M., Choobineh, S., Kordi, M. R., Rakhshan, K., 2025. Mitigating doxorubicin-induced hepatotoxicity in male rats: the role of aerobic interval training and curcumin supplementation in reducing oxidative stress, endoplasmic reticulum stress and apoptosis. Sci. Rep. 15. https://doi.org/10.1038/s41598-025-91133-6.